Lane-Change Detection Based on Vehicle-Trajectory Prediction

Hanwool Woo, Yonghoon Ji, Hitoshi Kono, Yusuke Tamura,
Yasuhide Kuroda, Takashi Sugano, Yasunori Yamamoto, Atsushi Yamashita, and Hajime Asama

***Abstract*—We propose a new detection method to predict a vehicle's trajectory and use it for detecting lane changes of surrounding vehicles. According to the previous research, more than 90% of the car crashes are caused by human errors, and lane changes are the main factor. Therefore, if a lane change can be detected before a vehicle crosses the centerline, accident rates will decrease. Previously reported detection methods have the problem of frequent false alarms caused by zigzag driving that can result in user distrust in driving safety support systems. Most cases of zigzag driving are caused by the abortion of a lane change due to the presence of adjacent vehicles on the next lane. Our approach reduces false alarms by considering the possibility of a crash with adjacent vehicles by applying trajectory prediction when the target vehicle attempts to change a lane, and it reflects the result of lane-change detection. We used a traffic dataset with more than 500 lane changes and confirmed that the proposed method can considerably improve the detection performance.**

***Index Terms*—Intelligent transportation systems, motion and path planning, recognition.**

I. Introduction

ACCORDING to a survey by the Japan Metropolitan Police Department, more than 90% of car crashes are caused by human errors [1]. Recently, autonomous car technologies and driving safety support systems have attracted considerable attention as solutions for preventing car crashes. The implementation of intelligent technologies to assist drivers in recognizing situations around their own vehicles can be expected to decrease the accident rates. Car crashes often occur when traffic participants attempt to change lanes [2]. If the safety support system of a vehicle can detect lane changes before other vehicles cross the centerline; accident rates can be significantly decreased.

Manuscript received September 7, 2016; accepted January 18, 2017. Date of publication January 27, 2017; date of current version February 16, 2017. This letter was recommended for publication by Associate Editor D. F. Wolf and Editor J. Wen upon evaluation of the reviewers' comments.

H. Woo, Y. Ji, H. Kono, Y. Tamura, A. Yamashita, and H. Asama are with the Department of Precision Engineering, Graduate School of Engineering, University of Tokyo, Tokyo 113-8656, Japan (e-mail: woo@robot.t.u-tokyo.ac.jp; ji@robot.t.u-tokyo.ac.jp; zin.robo@gmail.com; tamura@robot.t.u-tokyo.ac.jp; yamashita@robot.t.u-tokyo.ac.jp; asama@robot.t.u-tokyo.ac.jp).

Y. Kuroda is with the Mazda Motor Corporation, Yokohama 221-0022, Japan (e-mail: kuroda.y@mazda.co.jp).

T. Sugano and Y. Yamamoto are with the Mazda Motor Corporation, Hiroshima 730-8670, Japan (e-mail: sugano.t@mazda.co.jp; yamamoto.ya@mazda.co.jp).

Color versions of one or more of the figures in this letter are available online at http://ieeexplore.ieee.org.

Digital Object Identifier 10.1109/LRA.2017.2660543

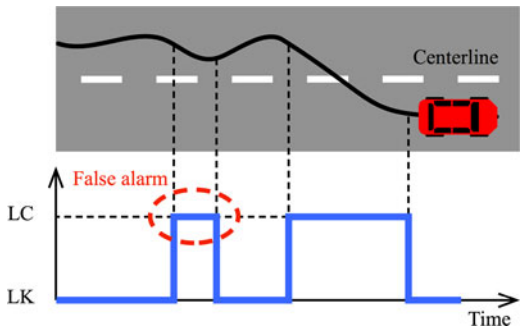

Fig. 1. Schematic illustration of false alarm caused by zigzag driving; previous methods have the problem of frequent false alarms. The graph at the bottom shows the detection result. LC denotes the state of lane changing, and LK denotes the state of lane keeping. We can see that LC was outputted during zigzag driving even though the vehicle did not change the lane.

For the detection of lane changes by other drivers, only measurable information from the outside should be used as features, and the selected features mainly determine the detection performance. Therefore, immeasurable features from the outside, such as steering angle, eye movement, and head motion [3]–[6], should be excluded. Schlechtriemen *et al.* suggested a detection method that uses only directly measurable information from the outside (e.g., lateral position, lateral velocity, and relative velocity) [7]. Mandalia and Salvucci suggested the use of the variance of the lateral position within a constant window size as a feature [8]. However, these methods have the problem of frequent false alarms caused by zigzag driving, as shown in Fig. 1. Here, a false alarm refers to a case in which the detection method determines a lane change when the vehicle does not change a lane, and this can result in the driver's distrust in the driving support system.

To decrease the number of false alarms that frequently occur when using previous methods, we propose a method to predict a vehicle's trajectory and use it for lane-change detection. Unlike previous methods that only use the past measurements until the current time, we focus on how human drivers predict a trajectory unconsciously. Our approach is to predict how other vehicles would move in certain scenarios and to extract information based on that prediction for use in lane-change detection. Most cases of zigzag driving are caused because of drivers aborting lane changes due to the presence of adjacent vehicles on the next lane. When a sufficient distance is not achieved with adjacent vehicles, drivers abort a lane change.

The proposed method considers the possibility of a crash with other vehicles, by using the potential field method. The potential field method has been generally applied to the navigation of mobile robots [9]–[11]. This method can generate a path that avoids contact with obstacles. Wolf and Burdick suggested a navigation method for an autonomous vehicle by applying the potential field method [12]. However, this method can only be used to calculate self-trajectory, as the desired velocity needs to be determined in order to calculate the potential energy. Tomar and Verma have suggested the trajectory method using a Support Vector Machine (SVM) and used it as the regression analysis method [13]. However, the method is able to predict only the lane changing trajectory not a lane keeping trajectory. As a result, their method cannot be applied without the method to detect lane changes beforehand. Houenou *et al.* proposed a vehicle-trajectory prediction method based on a motion model and a maneuver recognition model [14]. However, this method does not consider adjacent vehicles when it generates a trajectory. Therefore, an improper trajectory may be outputted in a crowded environment.

The contribution of the present research is as follows. Previous studies that deal with trajectory prediction have some limitations, as described in the previous paragraph. We propose a trajectory-prediction method that can be applied to other vehicles while considering the relationship with adjacent vehicles. It is able to predict a lane-changing trajectory and a lane-keeping trajectory. In addition, previous studies that deal with lane-change detection have the problem of frequent false alarms caused by zigzag driving. The proposed method is able to decrease the number of false alarms by using trajectory prediction. It is the first proposal to apply trajectory prediction to lane-change detection, and it demonstrates great performance.

II. Overview of Proposed Method

For improving detection performance, we propose a new method that predicts the trajectory of a target vehicle and uses it for lane-change detection. Fig. 2(a) shows the overview of our method. First, we have installed the sensor system in the primary vehicle as shown in Fig. 2(b). It consists of a position sensor (RT3003) and six laser scanners (ibeo LUX). The primary vehicle is able to acquire its position, the position of other vehicles, and the velocity of other vehicles by using these devices [15]. When these measurement values are inputted to the proposed method, it outputs whether the target vehicle would change the lane. We denote the output state of the proposed method by LC (lane changing) and LK (lane keeping). The proposed method consists of two parts: driving-intention estimation and vehicle-trajectory prediction.

The proposed method defines three types of features: the distance from the centerline, the lateral velocity, and the potential feature. We use the distance from the centerline instead of the lateral position to take account of the curvature of the road. The lateral velocity is calculated from the first derivative of the distance. The potential feature can describe situations at which a vehicle changes the lane by using the relative amounts with adjacent vehicles [16]. These features are converted to the feature

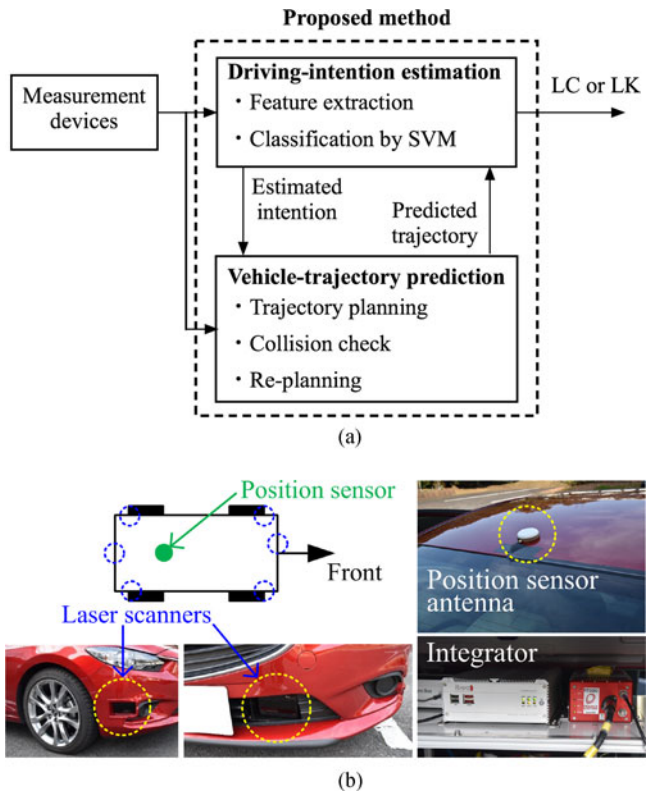

Fig. 2. Overview of proposed method: (a) when measurement values are inputted to the proposed method, it outputs whether the target vehicle would change the lane, (b) measurement devices in the primary vehicle.

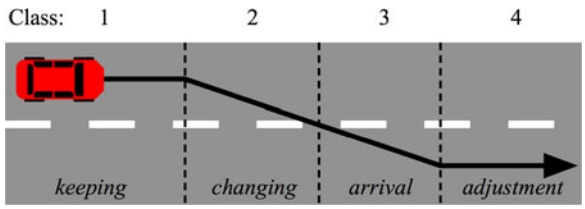

Fig. 3. Driving intentions.

vector that serves as the input of the driving-intention estimation model. The proposed method uses the SVM as the estimation model. We define that drivers have four intentions when they perform a lane change: *keeping*, *changing*, *arrival*, and *adjustment*, as shown in Fig. 3. Each driving intention is defined as a class, and the proposed method treats the driving-intention estimation as a multiclass classification problem. The extracted feature vector is inputted to the estimation model, following which the driving intention at the current time is determined. The method of driving-intention estimation is explained in detail in Section III.

The vehicle-trajectory prediction adopts the result of driving-intention estimation to identify the strategies that drivers may execute while driving. Generally, drivers execute different strategies with different driving intentions. When drivers have intentions such as *keeping* and *adjustment*, they aim at the front of the current lane and pay more attention to vehicles in the

same lane than vehicles in the other lanes. They may attempt to remain at the center of the lane. On the other hand, when drivers have intentions such as *changing* and *arrival*, they aim at the front of the next lane and must consider adjacent vehicles on not only the current lane but also the next lane. Therefore, in addition to the strategy, drivers must consider surrounding vehicles while driving. The proposed method uses the potential field method for trajectory planning and avoiding contact with surrounding vehicles. The goal, sidelines, and surrounding vehicles that generate potential energy are determined by following the driving intention. After planning, a collision check is conducted by updating the positions of other vehicles under the assumption that they move with constant velocity. If a collision with a surrounding vehicle occurs, the trajectory is re-planned. Then, the strategy is changed from *changing* to *keeping*, even though the estimated driving intention is *changing*. Such re-planning can be explained in a practical scenario as the abortion of a lane change due to the presence of adjacent vehicles. This re-planning in the driving-intention estimation can be expected to decrease false alarms caused by zigzag driving. The method of trajectory prediction is discussed specifically in Section IV.

III. Driving-Intention Estimation

A. Feature Extraction

For driving-intention estimation, we define the feature vector as consisting of the distance from the centerline, the lateral velocity, and the potential feature. The feature vector $\mathbf{x}_t$ at time t can be represented as

$$\mathbf{x}_t^{(k)} = \left[\mathbf{d}_\mathbf{t}^{(\mathbf{k})} \;\; \dot{\mathbf{d}}_\mathbf{t}^{(\mathbf{k})} \;\; \mathbf{p}_\mathbf{t}^{(\mathbf{k})}\right]^{\mathrm{T}} \tag{1}$$

$$\mathbf{d}_t^{(k)} = \left[d_{t-(W-1)}^{(k)} \;\; \ldots \;\; d_{t-1}^{(k)} \;\; d_t^{(k)}\right] \tag{2}$$

$$\dot{\mathbf{d}}_t^{(k)} = \left[\dot{d}_{t-(W-1)}^{(k)} \;\; \ldots \;\; \dot{d}_{t-1}^{(k)} \;\; \dot{d}_t^{(k)}\right] \tag{3}$$

$$\mathbf{p}_t^{(k)} = \left[p_{t-(W-1)}^{(k)} \;\; \ldots \;\; p_{t-1}^{(k)} \;\; p_t^{(k)}\right] \tag{4}$$

where k is an index that denotes the centerline. The proposed method can be adapted to both left lane changes and right lane changes. k is chosen based on the lane-changing side, and all features are calculated following the specified side. Since a lane change is a continuous process, rather than a temporary one, the feature vector must consider transitions of the features. We set a moving window to capture the transition, and W is the window size in (2)–(4). For example, $\mathbf{d}_t^{(k)}$ is a sequence that consists of W data until time t.

The curvature of the centerline is approximated by a second-degree polynomial using the least-squares method. Our system contains centerline information that includes the positions of all lane lines. The approximate curve at the kth line is

$$y^{(k)} = a_2^{(k)}(x^{(k)})^2 + a_1^{(k)}x^{(k)} + a_0^{(k)} \tag{5}$$

where $a_2^{(k)}$, $a_1^{(k)}$, and $a_0^{(k)}$ are coefficients at the kth line. The distance with respect to the kth line is defined as $d^{(k)}$, as shown in Fig. 4. The distance, $d^{(k)}$, is calculated by using the position

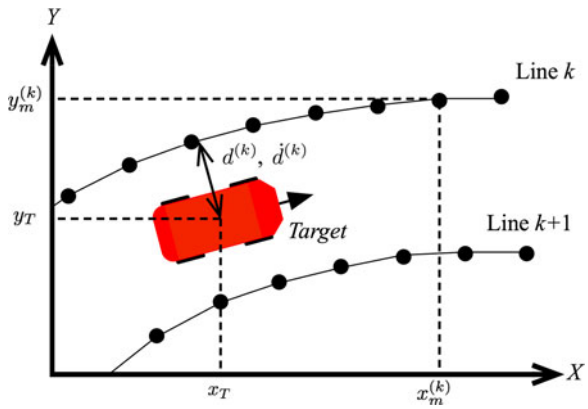

Fig. 4. Definition of features: $d^{(k)}$ and $\dot{d}^{(k)}$ are calculated by following the lane-changing side. For example, when the target vehicle changes the lane to the left lane, the centerline is chosen as the kth line in this figure.

of the target vehicle (x_T, y_T) and the kth approximate curve. We generate points at distance intervals of 0.1 m on the approximate curve and find the closest point from the target vehicle. The distance $d^{(k)}$ is calculated using

$$f(m) = \sqrt{(x_T - x_m^{(k)})^2 + (y_T - y_m^{(k)})^2} \tag{6}$$

$$d^{(k)} = \min\{f(m), m = 1, 2, ..., M\} \tag{7}$$

where m is an index of the generated point on the approximate curve, and M is the number of generated points. The distance, $d^{(k)}$, is defined as the first feature. The lateral velocity with respect to the centerline is calculated from the first derivative of the distance, $\dot{d}^{(k)}$. We define this value as the second feature. Because these features have units, in the absence of scaling, the estimation performance can be influenced by differences in units. Therefore, scaling should be conducted. We define the scaling value related to feature $d^{(k)}$ as half the width of the lane. The scaling value related to feature $\dot{d}^{(k)}$ is searched for during the training phase.

The third feature, the potential feature, is calculated using the ratio of the potential energy of the current lane to that of the next lane. We define the ratio of potential energy z as

$$z = \ln U_C - \ln U_N. \tag{8}$$

The value of p is calculated as

$$p = \varphi[z] \tag{9}$$

where $\varphi[\cdot]$ is the cumulative distribution function, U_C is the potential energy on the current lane, and U_N denotes the potential energy on the next lane. We define p as the potential feature and only consider four adjacent vehicles that are nearest to the target vehicle in each direction in each lane, as shown in Fig. 5. We define the target vehicle as *target*, a vehicle ahead of the target in the same lane as *preceding*, a vehicle behind the target in the same lane as *following*, a vehicle ahead of the target in the next lane as *lead*, and a vehicle behind the target in the next lane as *rear*. We denote these vehicles by capital letters (*T*, *P*, *F*, *L*, and *R*, respectively). Moreover, we define the region of interest of

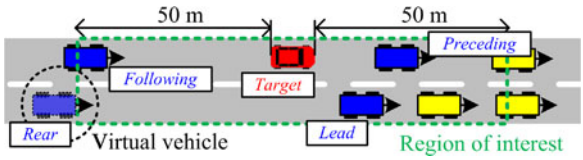

Fig. 5. Definition of adjacent vehicles for potential feature: the red vehicle represents the target vehicle, the blue vehicles represent the selected adjacent vehicles, and the yellow vehicles are not considered. The transparent blue vehicle represents the virtual vehicle that is set by the proposed method.

the *target* as a range that extends 50 m in each direction. When there is no vehicle in the region of interest, the proposed method sets a virtual vehicle that is 50 m away from the *target* with the same velocity. In Fig. 5, the virtual vehicle is set as the *rear*. The potential energy of each lane is derived by using

$$U_C = \omega_P U_P + \omega_F U_F \ (0 < U_C \leq 1) \tag{10}$$

$$U_N = \omega_L U_L + \omega_R U_R \ (0 < U_N \leq 1) \tag{11}$$

where ω_i is a weight coefficient at vehicle *i*. These coefficients determine which among the four adjacent vehicles affects the driver most significantly. Four adjacent vehicles generate a repulsive potential energy that is derived using

$$U_i = \frac{\exp[\eta(\Delta v_i)\cos\theta_i]}{2\pi I_0[\eta(\Delta v_i)]} \frac{\exp[-\frac{{r_i}^2}{2\sigma_i^2}]}{2\pi\sigma_i^2} \tag{12}$$

where *i* is a vehicle index, r_i is the relative distance, σ_i is the variance of r_i, Δv_i is the relative velocity, and θ_i is the relative angle. The first term in (12) represents the von Mises distribution, and $I_0(\cdot)$ is the modified Bessel function of order 0. By using the von Mises distribution, the drifted potential field can be generated considering not only the distance but also the relative velocity. The distribution is uniform when the parameter η is zero. If η is large, the distribution drifts toward the angle θ_i. In this research, η is adjusted by the relative velocity Δv_i, following which the drifting direction of the potential field is chosen as shown in Fig. 6. When vehicle i is faster than the *target*, a potential field drifting forward is generated in Fig. 6(a). Otherwise, when vehicle i is slower than the *target*, the distribution of the potential field is drifted backward in Fig. 6(b). Consequently, vehicle i does not interfere with the *target*. The potential feature represents the possibility of changing lanes through a comparison of situations between the current lane and the next lane.

Because noises might be added to measurements taken in the real world, noise filtering should be conducted before the feature extraction. The proposed method conducts noise filtering by using a Kalman filter and a moving average filter. The detailed methods and results are given in our previous works [15], [16].

B. Driving-Intention Estimation

The proposed method uses the SVM to classify the feature vector into the driving intention classes. The driving intentions may lie in a high-dimensional feature space, and the SVM kernel can address this problem through a conversion of features from

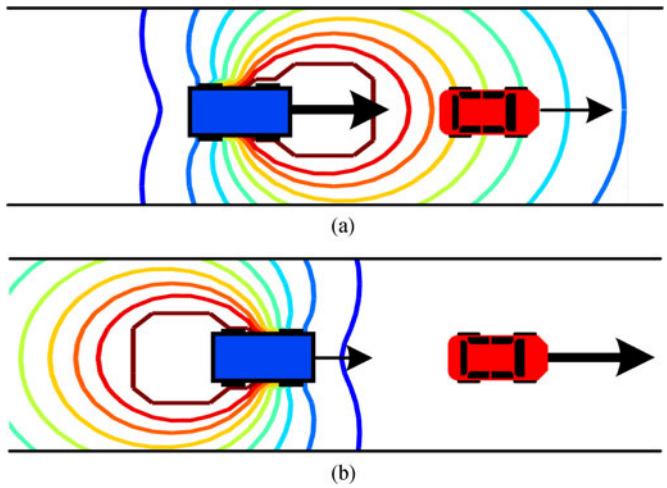

Fig. 6. Generated potential field depending on relative velocity: (a) the distribution of the potential field when vehicle i is faster than the *target*, (b) the distribution of potential field when vehicle i is slower than the *target*. The red vehicle is the *target*, and the blue one is vehicle i.

a low-dimensional space into a high-dimensional space [17]. The SVM determines the hyperplane parameters $\mathbf{w}$ and b that are used to classify the data:

$$y(\mathbf{x}) = \mathbf{w}^{\mathrm{T}}\phi(\mathbf{x}) + b \tag{13}$$

where $\phi(\mathbf{x})$ is the conversion function into the high-dimensional space. Using the training dataset, the limitation to the hyperplane parameter $\mathbf{w}$ can be set such that

$$t_n(\mathbf{w}^{\mathrm{T}}\mathbf{x}_n - b) \geq 1, \ (n = 1, ..., N) \tag{14}$$

where n represents the index of training data, and t_n is a class label at the feature vector $\mathbf{x}_n$. This limitation makes a margin in the range, $-1 < y(\mathbf{x}) < 1$. The SVM is a method that maximizes this margin, and this method gives reliable results in lane-change detection [8], [17]. The maximization of the margin can be represented as

$$\underset{\mathbf{w},b}{\operatorname{argmin}} \frac{1}{2}\|\mathbf{w}\|^2 \tag{15}$$

under the limitation in (14). This optimization problem can be solved by quadratic programming [18]. After the hyperplane parameters $\mathbf{w}$ and b are optimized, a new input can be classified using the trained model as following the sign in (13).

The performance achieved using the SVM strongly depends on kernel selection; however, because a kernel selection method has yet to be suggested, the only way to select the best kernel at present is through a process of trial and error. We selected the radial basis function as a kernel through trial and error. The radial basis function is defined by

$$K(\mathbf{x}, \mathbf{x}') = \exp(-g\|\mathbf{x} - \mathbf{x}'\|^2) \tag{16}$$

where g is the kernel parameter. The proposed method uses a simple approach for the multiclass extension of the binary SVM using a one-versus-all strategy. The driving intention at

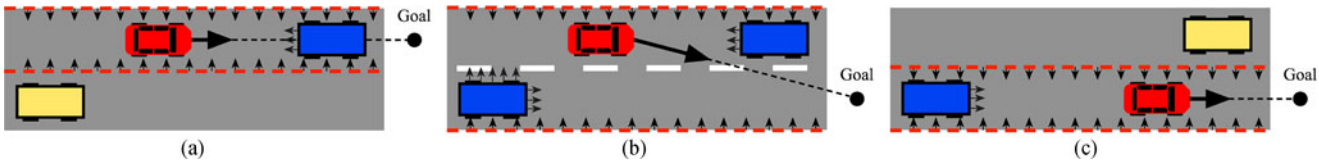

Fig. 7. Potential field generated by following driving intentions: (a) a case in which the driving intention is *keeping*, (b) a case in which the driving intention is *changing* and *arrival*, and (c) a case in which the driving intention is *adjustment*. The red vehicle represents the $target$, the blue one generates repulsive potential energy, and the yellow one does not generate repulsive potential energy. The red line denotes a sideline that generates repulsive potential energy.

the current time can be derived by

$$s_t = \underset{j}{\operatorname{argmax}}\, y_j(\mathbf{x}) \tag{17}$$

where j represents the number of classes. When the current-driving intention s_t is classified as *changing*, the proposed method judges that the *target* would attempt to change the lane.

IV. Vehicle-Trajectory Prediction

A. Trajectory Planning

The proposed method uses the potential field method to generate a trajectory of the *target* to a goal while avoiding adjacent vehicles. The potential field method used for trajectory prediction has no relationship with the potential feature. In trajectory prediction, the potential field method is just used to generate a path. This method generates attractive potential energy from the goal and repulsive potential energy from obstacles. In this research, we define three potential energies, and the total potential energy at the position (x, y) is derived as

$$U(x, y) = U_g + U_s + U_a \tag{18}$$

where U_g denotes the attractive potential energy from the goal, U_s denotes the repulsive potential energy from sidelines, and U_a denotes the repulsive potential energy from adjacent vehicles. First, the potential energy from the goal is calculated as

$$U_g(x, y) = -\omega_{g_x} x - \omega_{g_y} y \tag{19}$$

where ω_{g_x} and ω_{g_y} are the weight coefficients. The potential energy from the goal has a constant gradient. Second, the potential energy from sidelines is calculated as

$$U_s(x, y) = \omega_s \sum_k \exp\left[-\frac{(d^{(k)})^2}{\sigma_s^2}\right] \tag{20}$$

where ω_s is the weight coefficient, σ_s is the standard deviation of U_s, and $d^{(k)}$ is the distance from the kth sideline. Finally, the potential energy from adjacent vehicles is calculated as

$$U_a(x, y) = \omega_a \sum_{i=P,F,L,R} \exp\left[-\frac{(x - x_i)^2}{\sigma_{a_x}^2} - \frac{(y - y_i)^2}{\sigma_{a_y}^2}\right] \tag{21}$$

where i is the index of adjacent vehicles, ω_a is the weight coefficient, σ_{a_x} is the standard deviation of U_a in the X axis, and σ_{a_y} is the standard deviation of U_a in the Y axis. The force on the *target* at (x_T, y_T) can be calculated by

$$\mathbf{F}(x_T, y_T) = -\left[\frac{\partial U(x_T, y_T)}{\partial x} \quad \frac{\partial U(x_T, y_T)}{\partial y}\right]^{\mathrm{T}}. \tag{22}$$

The goal, sidelines, and adjacent vehicles that generate the potential energy are determined following the estimated-driving intention. First, when the driving intention is *keeping*, as shown in Fig. 7(a), the goal is set to the front of the current lane. The proposed method sets the goal to the center of the current lane. The left and right sidelines of the current lane generate repulsive potential energy, and they make the target vehicle keep a lane. The *preceding* and *following* vehicles generate repulsive energy. This potential energy makes the *target* keep a gap between front and back. However, the driver is not concerned with the vehicles on the next lane during lane keeping. Therefore, the *lead* and *rear* vehicles do not exert any forces on the *target*.

On the other hand, when the driving intention is *changing* or *arrival*, as shown in Fig. 7(b), the goal is set to the center of the next lane ahead. The goal generates the attractive potential energy indicated along the Y axis, in contrast to a case of lane keeping. The centerline between the current lane and the next lane does not generate repulsive potential energy. For example, when the *target* conducts a lane change to the right lane, the left sideline of the current lane generates repulsive potential energy. In contrast, the right sideline of the current lane does not participate, while the right sideline of the next lane generates repulsive potential energy. Lastly, the *lead* and *rear* vehicles generate repulsive potential energy. When a driver changes a lane, he may check the gap and relative velocity with vehicles on the next lane.

Lastly, when the driving intention is *adjustment*, as shown in Fig. 7(c), the goal is set to the center of the resultant lane ahead. The left and right sidelines of the resultant lane generate repulsive potential energy, and the *preceding* and *following* vehicles do not affect the force anymore. Only the *lead* and *rear* vehicles generate repulsive potential energy, as a result of which the *target* adjusts the velocity with them.

There is only one situation where a local minimum occurs in the proposed method. The situation occurs when adjacent vehicles are at a standstill, similar to a traffic jam. However, this situation can be eliminated when the adjacent vehicles start to move forward. As long as all vehicles are moving forward, a local minimum does not occur in the proposed method.

B. Collision Check & Re-Planning

The trajectory of the *target* is planned until the prediction time ϵ. The prediction time is defined as the elapsed time in the future at which trajectories are predicted. The proposed method assumes that adjacent vehicles drive with a constant velocity during the prediction time. Even if adjacent vehicles are

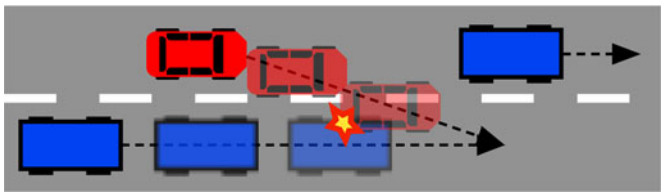

Fig. 8. Collision check: the proposed method considers the possibility of a crash between the $target$ and adjacent vehicles. The red vehicle is the $target$; blue ones are adjacent vehicles. Transparent color denotes the predicted position. If a collision occurs during a lane change, the predicted trajectory is re-planned.

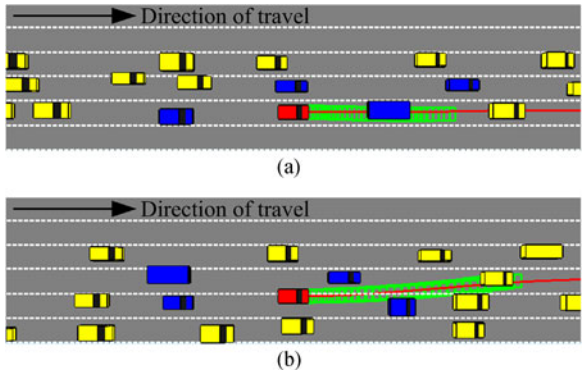

Fig. 9. Results of trajectory prediction (a) when the $target$ keeps the lane and (b) when the $target$ changes the lane. The green rectangle represents the predicted position at each time step, and the red line shows the ground truth. The red vehicle is the $target$, the blue ones are adjacent vehicles, and the yellow ones are other vehicles that are not considered.

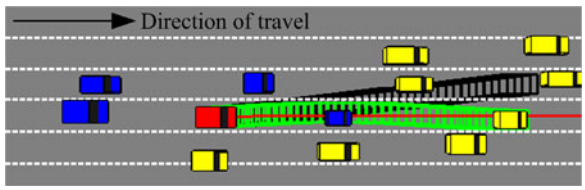

Fig. 10. Collision check and re-planning: the black rectangle represents the initially predicted trajectory. Re-planning was conducted because of the collision, and the green rectangle shows the re-planned trajectory. The red line shows the ground truth.

accelerating or decelerating, this action is prominently reflected in the next time step because the trajectory prediction is performed at each time step. This update of position is conducted to check the possibility of collision between the *target* and adjacent vehicles, as shown in Fig. 8. If a collision occurs during a lane change, the predicted trajectory is initialized and re-planned. The potential field is re-generated based on the strategy, *keeping*, even if the estimated driving intention was *changing*. This strategy can be explained as the abortion of a lane change by a driver when he/she feels unsafe because of the insufficient gap or velocity. This strategy is expected to eliminate false alarms caused by zigzag driving.

The proposed method extracts the features based on the predicted trajectory for use in lane-change detection. The extracted features are applied as the future measurement, and the driving intention is re-estimated using the features. Finally, the proposed method outputs LK or LC. When the re-estimated driving intention is *keeping* or *adjustment*, LK is outputted. Otherwise, when the re-estimated driving intention is *changing* or *arrival*, LC is outputted.

V. Experimental Results

We trained and tested the proposed method using a real traffic dataset published by the Federal Highway Administration of the United States [19]. The dataset was collected on eastbound I-80 in the San Francisco Bay Area. The measurement area was approximately 500 m in length and consisted of six freeway lanes. The dataset consisted of measurements taken per 0.1 s for 15 min, for a total of three times. Data from 5,678 vehicles were collected. Among them, we used 300 lane-change data for the training and 523 lane-change data for the test.

A. Evaluation of the Vehicle-Trajectory Prediction

We confirmed that the trajectory of the *target* was properly predicted. The parameters should be evaluated to consider how they balance with one another in order to avoid collisions with other vehicles. Parameter imbalance can be a cause of collisions with other vehicles, in addition to causing an unstable trajectory in the lateral direction. Therefore, parameter values largely determine the accuracy of a trajectory prediction. The parameters were manually tuned in order to obtain the minimum error of trajectory prediction during lane changes. As a result, the parameters have been set to the following values: $\omega_{g_x} = 0.5$, $\omega_{g_y} = 1.0$, $\omega_s = 2.0$, $\sigma_s = 1.1$, $\omega_a = 12.2$, $\sigma_{a_x} = 5.0$, and $\sigma_{a_y} = 17.4$. The prediction time has been determined by the detection performance and the computation. A short prediction time is not sufficient for the collision check. In contrast, long prediction time requires additional computation and does not ensure improved detection performance. We considered the balance and have determined that $\epsilon = 2.0$ s. The prediction was conducted with a time step of 0.1 s. Moreover, the proposed method should satisfy the computation limit derived from the sensor system. Our sensor system has an update rate of 32 Hz; therefore, lane-change detection, including trajectory prediction, must be updated earlier than the sensors. We confirmed that the update rate of the proposed method is 56 Hz on average, the maximum rate is 77 Hz, and the minimum rate is 36 Hz using the complete testing dataset. This means that the proposed method is able to satisfy the system requirement. Fig. 9 shows the results in one case from the test dataset. The red vehicle is the *target*, the green rectangle represents the predicted position at each time step, and the red line shows the ground truth. Fig. 9(a) shows the result at a point when the *target* kept the current lane; Fig. 9(b) shows the result at a point when the *target* conducted a lane change. We can see that the predicted trajectory was quite consistent with the ground truth. In Fig. 9(b), the *target* followed the *lead* vehicle smoothly, and a collision did not occur because the *lead* vehicle was faster than the *target*.

Fig. 10 shows a case of collision check and re-planning. The black rectangle represents the canceled trajectory because collision was predicted. In this case, the driving intention was

TABLE I
RESULT OF LANE CHANGE DETECTION

Without trajectory prediction				Proposed method	
		Detection result		Detection result	
		LC	LK	LC	LK
Ground Truth	LC	523	0	523	0
	LK	36	487	17	506

TABLE II
PERFORMANCE COMPARISON WITH PREVIOUS METHODS

Method	Precision	Recall	F_1	τ_d
Mandalia [8]	80.0 %	81.1 %	80.5 %	1.33 s
Schlechtriemen [7]	93.6 %	99.3 %	96.4 %	1.65 s
Proposed method	96.3 %	100 %	98.1 %	1.74 s

estimated as *changing*; however, the relative velocity with respect to the *lead* vehicle was not sufficient. As a result, the driver stopped to change the lane. Such situations have been the main cause of false alarms, and from the results, we qualitatively confirm that the proposed method properly eliminated a false alarm in spite of the zigzag driving. The proposed method re-planned the trajectory as *keeping* the current lane even though the driving intention was initially estimated as *changing*. Through this collision check and re-planning, the proposed method is able to reduce false alarms.

B. Criteria of Performance Evaluation

We used two evaluation criteria: the detection time, τ_d, and the detection accuracy, F_1 score. First, we defined the detection time as

$$\tau_d = \tau_c - \tau_j, \tag{23}$$

where τ_c is the moment at which the *target* crosses the centerline, and τ_j is the moment at which the proposed method judges that the *target* would change the lane. A large value of τ_d indicates a high early detection performance. We defined the following criteria using the detection time τ_d:

1) *Success:* $0 < \tau_d < 5.0$ (judged within the time limit).
2) *Failure:* $\tau_d \leq 0$ (judged too late).
3) *False alarm:* $\tau_d \geq 5.0$ (judged too early).

Generally, a lane change takes 3.0 to 5.0 s according to previous research [20]. Accordingly, we judged cases in which $\tau_d \geq 5.0$ s as false alarms.

Second, the F_1 score is defined as

$$F_1 = 2 \times \frac{\text{precision} \times \text{recall}}{\text{precision} + \text{recall}}. \tag{24}$$

Including precision in the F_1 score allows for the evaluation of the false-alarm rate when the proposed method judges a case in which the vehicle does not change a lane as an incorrect lane change, and recall represents the failure rate, the most dangerous case, in which the proposed method judges a case that should be a lane-changing case as a lane-keeping case. The lane-change estimation method must satisfy recall with 100% accuracy.

C. Evaluation of Detection Performance

We evaluated the detection performance of the proposed method by using the entire testing dataset. First, Table I lists the results of detection accuracy. To evaluate the effectiveness of trajectory prediction, we compared the results with those obtained from a method that is identical except that trajectory prediction is not applied. We can see from the table that the trajectory prediction reduced the false-alarm cases from 36 to 17. Almost 53% of false-alarm cases were reduced by applying the proposed method. Fig. 11 shows the result of one case from the entire testing dataset. The two methods used the same features, as shown in Fig. 11(a). The blue line represents the distance from the centerline, the green line shows the lateral velocity, and the red line shows the potential feature. Considering the blue line, we find that zigzag driving occurred near $t = 20$ s. Fig. 11(b) shows the driving intention estimated by the method performed without the trajectory prediction. A false alarm occurred at $t = 20$ s because of the zigzag driving. On the other hand, the proposed method eliminated the false alarm, as shown in Fig. 11(c). From these results, we can confirm that the trajectory prediction can prevent false alarms and improve the performance of lane-change detection.

In addition, we compared the performance of the proposed method with the performance of two previous methods. The first of these methods uses the variance of the lateral position predicted at 0 m, 10 m, 20 m, and 30 m ahead within a constant window size as features [8]. This method also uses the SVM as a classification method. The second method uses the lateral position, the lateral velocity, and the relative velocity of the *preceding* vehicle [7]. This method uses the Bayes algorithm that estimates the driving intentions. We implemented these previous methods and evaluated them using the same testing dataset. Table II lists the results in terms of the average precision, recall, F_1 score, and detection time τ_d. We can see from the table that the proposed method outperforms previous methods in terms of both accuracy and early detection. Specially, the proposed method detected all of the lane changes correctly; thus, the recall was 100% accurate . In contrast, the previous methods failed to detect several lane-changing cases, because of which dangerous cases can occur without any warning given to the driver. We consider that one of the causes of detection failure is the use of variance as a feature in the first method. In the case of lane changes conducted slowly, the variance of the lateral position has a small value, because of which there is a possibility that the cases cannot be detected. The second method considers only the situation in which the *preceding* vehicle is slower than the *target*. Thus, other situations may be at the risk of not being detected. Moreover, the two methods have an aspect in common that adjacent vehicles are not considered on the next lane. Consequently, false alarms frequently occur in comparison with the proposed method. From above results, we can confirm that the proposed method dramatically improves performance in terms of both accuracy and early detection.

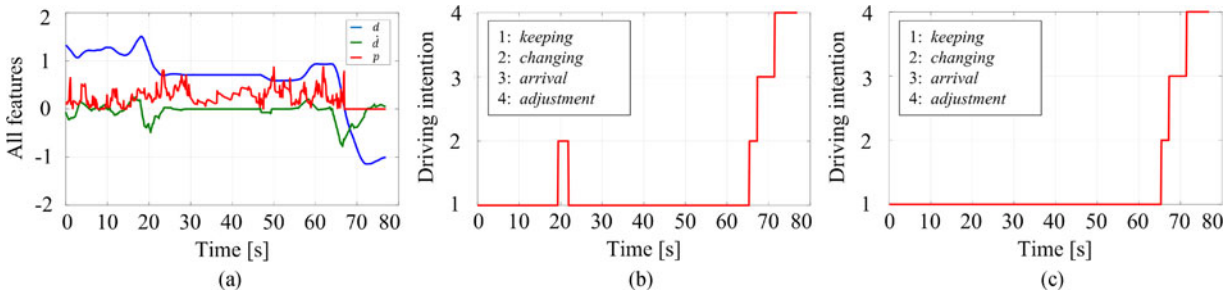

Fig. 11. Evaluation result of lane-changing case: (a) record of all features that are normalized, (b) driving intention estimated by the method without trajectory prediction, and (c) the driving intention estimated by the proposed method.

VI. Conclusion

In this research, we proposed a new lane-change detection method based on vehicle-trajectory prediction. Previous methods have the problem of frequent false alarms caused by zigzag driving that can result in user distrust in the driving support system. Through comparison with previous methods, we confirmed that the proposed method with vehicle-trajectory prediction can reduce false alarms. In addition, the method can detect a lane change, on average, 1.74 s before the target vehicle crosses the centerline with 98.1% accuracy. We demonstrated that the proposed method outperforms previous methods in terms of the accuracy and early detection. The reason for improvement is expected to be due to the fact that the proposed method considers adjacent vehicles on the next lane, while previous methods do not.

As future work, we have continuously evaluated other variables that might affect driving intentions and are expected to improve the performance (e.g., traffic density, types of vehicles).

References

[1] Japan Metropolitan Police Department, "States of occurrence of traffic accidents," TMPD, Tokyo, Japan, 2014.
[2] U.S. Department of Transportation, "Lane change/merge crashes: Problems size assessment and statistical description," U.S. DOT, Washington, DC, USA, Rep. DOT HS 808 075, 1994.
[3] R. Dang, F. Zhang, J. Wang, S. Yi, and K. Li, "Analysis of Chinese driver's lane change characteristic based on real vehicle tests in highway," in *Proc. IEEE Int. Conf. Intell. Transp. Syst.*, 2013, pp. 1917–1922.
[4] N. Kuge, T. Yamamura, O. Shimoyama, and A. Liu, "A driver behavior recognition method based on a driver model framework," SAE, Warrendale PA, USA, Tech. Rep. 2000-01-0349, 2000.
[5] G. Li, S. E. Li, Y. Liao, W. Wang, B. Cheng, and F. Chen, "Lane change maneuver recognition via vehicle state and driver operation signals-results from naturalistic driving data," in *Proc. IEEE Int. Conf. Intell. Veh. Symp.*, 2015, pp. 865–870.
[6] A. Doshi and M. M. Trivedi, "On the roles of eye gaze and head dynamics in predicting drivers intent to change lanes," *IEEE Trans. Intell. Transp. Syst.*, vol. 10, no. 3, pp. 453–462, Sep. 2009.
[7] J. Schlechtriemen, A. Wedel, J. Hillenbrand, G. Breuel, and K. D. Kuhnert, "A lane change detection approach using feature ranking with maximized predictive power," in *Proc. IEEE Int. Conf. Intell. Veh. Symp.*, 2014, pp. 108–114.
[8] H. Mandalia and D. Salvucci, "Using support vector machine for lane-change detection," in *Proc. IEEE Int. Conf. Human Factors Ergonomics Soc.*, 2005, pp. 1965–1969.
[9] H. Chiang, N. Malone, K. Lesser, M. Oishi, and L. Tapia, "Path-guided artificial potential fields with stochastic reachable sets for motion planning in highly dynamic environments," in *Proc. IEEE Int. Conf. Robot. Autom.*, 2015, pp. 2347–2354.
[10] V. A. M. Jorge *et al.*, "Ouroboros: Using potential field in unexplored regions to close loops," in *Proc. IEEE Int. Conf. Robot. Autom.*, 2015, pp. 2125–2131.
[11] Y. Ma, G. Zheng, W. Perruquetti, and Z. Qiu, "Motion planning for non-holonomic mobile robots using the i-PID controller and potential field," in *Proc. IEEE/RSJ Int. Conf. Intell. Robots Syst.*, 2014, pp. 3618–3623.
[12] M. T. Wolf and J. W. Burdick, "Artificial potential functions for highway driving with collision avoidance," in *Proc. IEEE Int. Conf. Robot. Autom.*, 2008, pp. 3731–3736.
[13] R. S. Tomar and S. Verma, "Trajectory prediction of lane changing vehicles using SVM," *Int. J. Veh. Safety*, vol. 5, no. 4, pp. 345–355, 2011.
[14] A. Houenou, P. Bonnifait, V. Cherfaoui, and W. Yao, "Vehicle trajectory prediction based on motion model and maneuver recognition," in *Proc. IEEE Int. Conf. Intell. Robots Syst.*, 2013, pp. 4363–4369.
[15] H. Woo *et al.*, "Lane-changing feature extraction using multisensor integration," in *Proc. 16th Int. Conf. Control, Autom. Syst.*, 2016, pp. 1633–1636.
[16] H. Woo *et al.*, "Automatic detection method of lane-changing intentions based on relationship with adjacent vehicles using artificial potential fields," *Int. J. Automot. Eng.*, vol. 7, no. 4, pp. 127–134, 2016.
[17] P. Kumar, M. Perrollaz, S. Lefevre, and C. Laugier, "Learning based approach for online lane change intention prediction," in *Proc. IEEE Int. Conf. Intell. Veh. Symp.*, 2013, pp. 797–802.
[18] K. P. Bennett and E. J. Bredensteiner, "Duality and geometry in SVM classifiers," in *Proc. 17th Int. Conf. Mach. Learn.*, 2000, pp. 57–64.
[19] The Federal Highway Administration, "Next generation simulation," 2015. [Online]. Available: http://ops.fhwa.dot.gov/trafficanalysistools/ngsim.htm. Accessed on: May 10, 2015.
[20] T. Toledo and D. Zohar, "Modeling duration of lane changes," *Transp. Res. Rec., J. Transp. Res. Board*, vol. 1999, pp. 71–78, 2007.